


RESEARCH ARTICLE

Open Access

Universat-SOCRAT multi-satellite project to study TLEs and TGFs



Mikhail Panasyuk^{1,2}, Pavel Klimov^{1*} , Sergei Svertilov^{1,2}, Alexander Belov^{1,2}, Vitali Bogomolov^{1,2}, Andrei Bogomolov¹, Gali Garipov¹, Anatoly Iyudin¹, Margarita Kaznacheeva¹, Ivan Maksimov¹, Alexander Minaev^{1,2}, Artem Novikov^{1,2}, Pavel Minaev³, Vasili Petrov¹, Alexei Pozanenko^{3,4}, Yan Shtunder^{1,2} and Ivan Yashin¹

Abstract

We present concept of a new multi-satellite Universat-SOCRAT project aimed to study transient phenomena in the upper atmosphere such as transient luminous events (TLEs) and terrestrial gamma-ray flashes (TGFs). It is a new space project of Lomonosov Moscow State University based on the use of a few satellites in the near-Earth orbit for real-time monitoring of radiation environment, natural (asteroids, meteoroids) and artificial (space debris) potentially dangerous objects, electromagnetic transients including cosmic gamma-ray bursts, terrestrial gamma-ray flashes, and optical and ultraviolet bursts in the Earth's atmosphere.

Study of TLEs and TGFs remains an important and demanding task despite of a multitude of recently acquired data for these phenomena. This might be explained by the absence of comprehensive theoretical understanding of physical nature of high-energy processes in the Earth's atmosphere. Multi-wavelength synchronous observations with moderate accuracy of localization of TGF and TLE events are necessary to gain an insight of physics governing these high-energy processes in the Earth's atmosphere. In the article, we present results of TLE observations in space experiments of Moscow State University and discuss advanced instruments for optical observations of TLEs, as well as gamma-ray burst monitor and tracking gamma spectrometer for TGFs observations.

Keywords: Electromagnetic transients, TLE, TGF, Imager, Track spectrometer

Introduction

One of the main problems of modern geoscience and atmospheric physics in particular is understanding the nature of the so-called transient atmospheric events (TAE), which include terrestrial gamma-ray flashes (TGFs) and transient luminous events (TLEs). TGFs and TLEs are observed both in the stratosphere and mesosphere, i.e., at the source altitude from about 12 km up to a few dozen kilometers (Cummer et al. 2014). Electromagnetic transient phenomena in the upper atmosphere are global in nature and associated with electric discharges. During the electric discharges between the clouds and the clouds and ionosphere (altitudes from 5–10 km to 60–90 km) short-time bursts of electromagnetic radiation,

with duration from fractions of millisecond up to several hundred of milliseconds, within wide spectral range from visual light up to UV, and even X-rays and gamma-rays, are observed.

TLEs are optical flashes known as sprites, elves, and blue jets. Their parameters including spatial and temporal structure, rate of occurrence, and optical brightness in different ranges could be found in (Vaughan and Vonnegut 1989; Fisher 1990; Lyons 1994; Boeck et al. 1995; Winckler et al. 1996; Boccippio et al. 1995).

TGFs are extremely short gamma-ray events, which were discovered by BATSE experiment on-board Compton Gamma-Ray Observatory ((Fishman et al. 1994)). Since 1991 up to 2000, 36 TGFs were discovered, some of them were associated with thunderstorms. Later, these observations were confirmed by the space observatory RHESSI (Smith et al. 2005). The largest TGF statistics was obtained by Fermi space gamma observatory that was launched in 2008. To the present, more than 2700

*Correspondence: pavel.klimov@gmail.com

¹Skobeltsyn Institute of Nuclear Physics, Lomonosov Moscow State University, 1(2), Leninskie gory, Moscow 119991, Russia

Full list of author information is available at the end of the article

TGFs have been detected in the 10 keV–40 MeV energy range, the average detecting frequency is one burst in ~ 4 days (Briggs et al. (2013); Roberts et al. (2018)). The TGFs were also studied during AGILE (Tavani et al. (2011)), and INTEGRAL (Minaev et al. 2014; Minaev and Pozanenko 2018 and Vernov (Bogomolov et al. 2017)) space missions.

TGFs and TLEs might be the consequence of physical processes resulting from different kinds of high-energy release over short time intervals (between 10^{-6} and 10^{-3} s). It is supposed that TGFs could accompany a particular type of a lightning activity (upward positive intra-cloud (IC) lightning) (Dwyer et al. (2012)). The other manifestation of energetic processes during thunderstorm activity is upward travelling of relativistic run-away electron beams at the altitudes of 60–80 km (Bell et al. (1995); Lehtinen et al. (1997)). Electrons with energies of ~ 1 MeV and higher are able to penetrate through the upper atmosphere, up to the Earth's magnetosphere, and finally into radiation belts. However, attempts of direct measurements of runaway electrons by means of large area electron detector on-board Tatiana-2 satellite did not show any tangible results (Sadovnichy et al. (2011)). Nevertheless, detection of electrons from the CGRO/BATSE (Dwyer et al. (2008)) and positrons from the GBM/Fermi (Briggs et al. 2011) space missions may be considered as indirect evidence of the occurrence of runaway electron avalanches taking place in the area of thunderstorm activity. According to these results, positron portion can reach up to 11% of these up-going beams by different estimations (Briggs et al. (2011)).

So despite more than 20 years of experimental and theoretical research of TAE, there are no clear interpretations of such phenomena. Study of TLEs and TGFs is very important for understanding of their physical nature and verification of theoretical models. Simultaneous observations at different electromagnetic wave bands with, at least, moderately good accuracy of event localization are necessary to gain an insight of physics governing these high-energy processes in the Earth's atmosphere. Also multi-messenger observation, i.e., detection of neutrons, electrons probably connected with TGF source, can provide us direct information about acceleration mechanisms in the TGF source. As for TLEs, most of such phenomena are well-known as a specific kind of thunderstorm activity. Nevertheless, some events were observed far from thunderstorm areas. The nature of such non-usual transients is still unknown, thus further observations of TLEs are also necessary.

In this article, we present concept of a new multi-satellite Universat-SOCRAT space project of Lomonosov Moscow State University based on the use of a few satellites in the near-Earth space for real-time monitoring of radiation environment, natural (asteroids,

meteoroids) and artificial (space debris) potentially dangerous objects, electromagnetic transients including cosmic gamma-ray bursts, terrestrial gamma-ray flashes, and optical and ultraviolet bursts in the Earth's atmosphere.

The problem of TLE and TGF study in modern space missions

The common point is that transient atmospheric events are caused by discharges related to thunderstorm activity. Thus, most frequent TLEs—elves—are caused by the electromagnetic pulse (EMP) from lightning or powerful intracloud discharge. Another type of TLE—sprites—is a mesospheric phenomenon associated usually with positive cloud-to-ground lightning discharge, and is caused by a quasi-electrostatic field ((Pasko et al. 2012)).

The model of relativistic runaway electron avalanches (RREA) based on the runaway electron breakdown (REB), predicted in 1992 and studied theoretically in details by (Gurevich et al. 1992) and (Dwyer et al. 2012), is often used for interpretation of TGF. The typical feature of REB is its occurrence at electric fields lower than typical breakdown field in the cloud, with the seed electrons presence, that are necessary for its initiation. An alternative approach supposes electron multiplication during its acceleration, which is considered within the relativistic feedback discharge (RFD) model (Dwyer (2007)). This model assumes acceleration of thermal electrons up to relativistic energies that needs a very high accelerating electric field ~ 280 kV/cm. It is possible for run-away electrons produced by lightning current pulse in a strong field near lightning step-leader streamer and edges ((Moos and Moos 2006)). Due to a large number ($\sim 10^{12}$) of cold electrons, relatively small ($\sim 10^5 - 10^6$) multiplication factor in avalanche is sufficient for gamma-ray flash generation. Duration of coronal streamer discharge on the one step of lightning leader is very short (~ 10 μ s); however, due to Compton scattering duration of gamma-ray flashes at satellite, altitudes can be ~ 50 μ s (Østgaard et al. (2008)).

Current experimental data on discharges in the upper atmosphere have shown that these phenomena are global. A number of discharges and the energy released in these discharges are so high that we can expect certain correlation between the discharges and other geophysical phenomena. Physical mechanisms leading to TGFs and TLEs at optical and gamma-ray ranges can be different. The Universitetsky-Tatiana, Tatiana-2, and Vernov mission data demonstrated cogently the appearance of TLEs types, which are not associated with thunderstorm activity (Sadovnichy et al. (2011); Sadovnichy et al. (2007); Klimov et al. (2018)). Below we present the results of TLE observations during these experiments and discuss the problem of TLE and TGF study during modern space missions.

Results of TLE observations in space experiments of Moscow State University

UV fluorescence detectors were put on boards of several MSU micro-satellites in order to understand the transient events as a geophysical problem of global electric circuit better. These include “Universitetsky-Tatiana” (Sadovnichy et al. (2007); Garipov et al. (2005)), “Universitetsky-Tatiana-2” (Sadovnichy et al. (2011); Vedenkin et al. (2011); Garipov et al. (2013)), and “Vernov” (Panasyuk et al. 2016a,b).

These satellites were equipped with a simple wide-field UV (240–400 nm) and near infrared (NIR) (600–800 nm) detectors (DUV). Detectors consist of two photomultiplier tubes (PMT) Hamamatsu R1463 with multi-alkali cathode, UV transparent entrance window, and electronics module, which allows to observe transient flash profiles. The field of view (FOV) 16° of every detector is limited by a collimator. The detectors provided measurements of atmospheric emission with 1 ms (Tatiana-2) and 0.5 ms (Vernov) temporal resolution. The detailed description for DUV electronic module and measurements is presented in (Sadovnichy et al. 2007) and (Garipov et al. 2006). For observation from space, transient UV events generated in the upper atmosphere are at favorable conditions, as they are less absorbed in route from event to detector.

Data from DUV are registered as UV temporal profiles from transients observed from nadir direction within 16° FOV. They demonstrate a variety of temporal structures ranging from a single peak to quite complicated profiles. Short events with about 1 ms duration are the most numerous and can be associated with elves, while series of flashes can be interpreted as multiple lightning discharges, or sequences of lightning and TLEs (sprites, jets, etc.). Number of events without NIR signal at all were observed. These dim transients, which have only signal in UV range, might be discharges at the “pre-lightning” stage, which do not always develop to the lightning stage, or, alternatively, can be low-altitude TLEs, like blue jets and blue starters (Klimov et al. (2017)).

Other events that have signal in both UV and NIR bands belong to the transients as well, but could not be associated with lightning itself. This conclusion is based on temporal structure of events and their spectrum that is different from the lightning spectrum (measured in (Orville and Henderson 1984) and are more like the sprite spectrum (Milikh et al. (1998)). The analyses of event altitude based on UV to IR ratio in these experiments were made by (Garipov et al. 2013) and (Klimov et al. 2017). For more reliable conclusions on the nature of luminous transients, the study of lightning and of other types TAE spectra is needed, especially in UV range.

As was earlier mentioned by (Garipov et al. 2013), some events detected on-board Tatiana-2 have occurred

not above clouds, and rather far from the thunderstorm regions. The recent analyses of such events by instruments on-board Vernov satellite was made by Klimov et al. 2018, where these events were compared with the data of ground-based lightning location networks and with satellite data of the cloud coverage, and as a result of this analysis, a new class of far-from-thunderstorm events was suggested. But no hypotheses of their nature was put forward, or even suggested. More information on the spectral and spatial distributions of such events is needed in order to understand their origin and nature.

Important and new result is that in both experiments Tatiana-2 and Vernov, TAE from the large thunderstorm regions were regularly observed as a series of events registered in every period T , technically the smallest possible period between registered events. An example of such series detected by DUV on-board the Vernov satellite is shown in Fig. 1. Here, values of maximum signal in one bin of the oscilloscope trace, triggered every 4.5 s, are shown. Blue and red lines correspond to UV and NIR wave bands, respectively. The average rate of lightning available from LIS (lightning imaging sensor) data (Christian et al. 1999) for the thunderstorm region is much lower than the observed transient rate in the series. Moreover, in some series, TAE are observed in clear atmosphere, no clouds conditions, which is speaking against lightning origin of those TAE. Analysis of correlation between clouds and any TAE (in series or not) is also contradict to the lightning origin of some TAE. An equal number of transients from both cloudy and cloudless areas of the atmosphere (Vedenkin et al. 2011; Garipov et al. 2013) were observed, while lightning is strongly correlated with clouds. Those data should be confirmed by new measurements with better identification of TAE and lightning.

Recently, a new instrument—detector TUS—was launched on-board the Lomonosov spacecraft. This detector is a mirror telescope with a large aperture (2 m^2) which provides a high sensitivity of the detector. It is important to note that it has a spatial resolution of 5 km in the atmosphere observing the total area of $80 \times 80 \text{ km}^2$. The detailed description of the TUS detector is presented in (Klimov et al. 2017) and first results of measurements in (Khrenov et al. 2017).

The TUS detector can be operated in four modes selected to detect various fast optical phenomena that happen in the atmosphere at different time scales and with different time sampling. The main mode has a time sampling of $0.8 \mu\text{s}$. This mode is efficient for elve measurements, the most common type of transient luminous events. Three other modes have time sampling of $25.6 \mu\text{s}$ and 0.4 ms for studying TLEs of different kinds slower than elves, namely, for sprites, blue jets, gigantic jets, etc., and 6.6 ms for detecting thunderstorm activity at a longer time scale of $\sim 1.7 \text{ s}$.

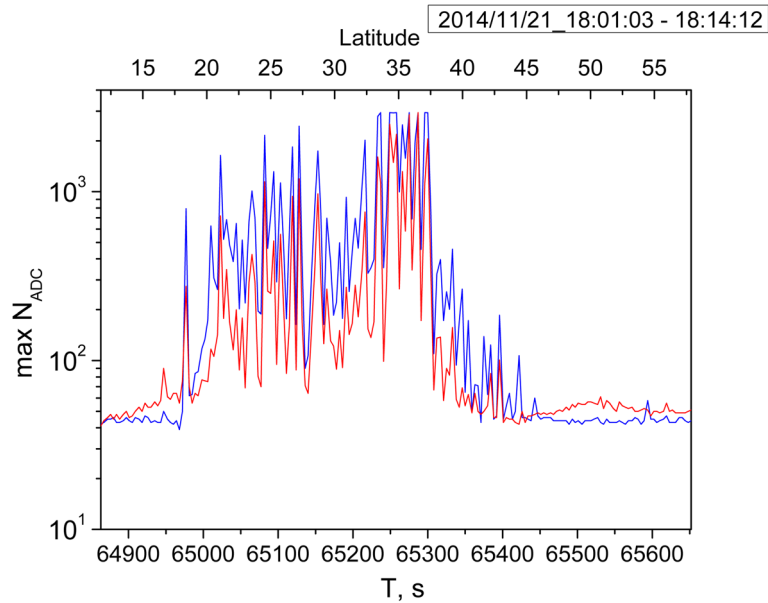


Fig. 1 Example of series of TAE in the Vernov experiment (blue curve—UV emissions; red—infrared one)

The advantage of the detector is that its spatial resolution allows us to identify some types of TLEs, for example, elves. An arc-like shape of the track made by the brightest PMTs can be seen in Fig. 2, and short duration of the signal (waveforms in Fig. 3) prove the hypotheses that this event corresponds to elve detection.

Another interesting result for the serial flashes was observed in the fourth timing mode. The example of such series is shown in Fig. 4. It has a long waveform of 1.7 s duration with a few dozen of peaks. This sequence

of flashes has very complicated temporal structure with numerous peaks and was detected from a thunderstorm region. It is interesting to note that similar series were observed far from the thunderstorm regions as well, but peaks for these series have longer duration. Analysis of these data is still in progress.

TUS detected TLEs demonstrate the advantages of using detector with high temporal resolution, spatial resolution, also capable to record a long time series. Unfortunately, due to Lomonosov telemetry limits, the detector

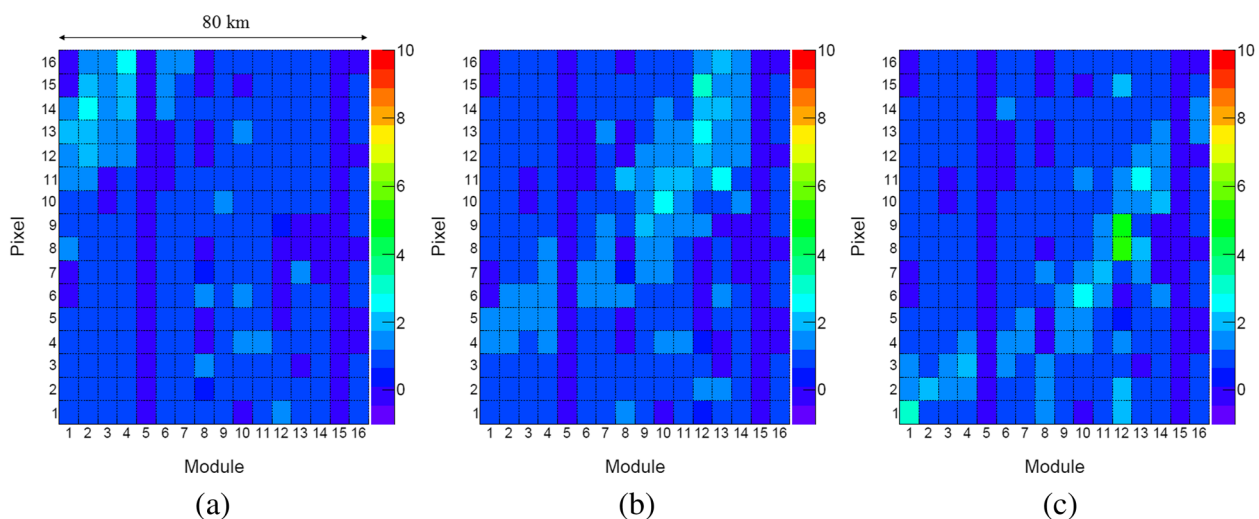


Fig. 2 Snapshots of the focal plane show arc-like shape and movement of the pattern through the detector's field of view. The snapshots were taken at $t = 0.077$ ms (a), 0.174 ms (b), and 0.182 ms (c) from the beginning of the record. The signal amplitude is color coded in arbitrary units and scaled to individual PMT gain

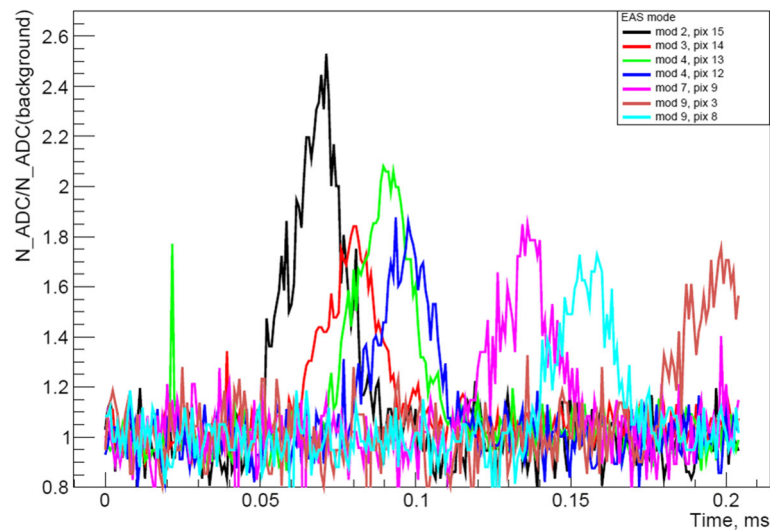


Fig. 3 Waveforms of several hit pixels of the elves type event registered on September 18, 2016 above continental Africa. The Y-axis is a ratio of ADC counts and background signal for each pixel

can record only one event per minute, having a huge dead time between events, and therefore, four modes with different temporal resolutions were used separately and not simultaneously.

The TLE and TGF study in other missions

At least three space projects TARANIS (Blanc et al. (2007)), ASIM (Neubert et al. (2006)), and TRYAD ((Briggs et al. 2015)) are intended for complex studies of the high-energy phenomena in the atmosphere, including TLEs and TGFs. The ASIM mission was successfully launched in April 2018, while TARANIS and TRYAD should be realized in the near future.

The TARANIS (Tool for the Analysis of RAdiations from lightNING and Sprites) project with its claimed goals, tasks, and methods is very similar to the Russian space mission Vernov that was operated in space during the second half of 2014 (Panasyuk et al. 2016a,b). TARANIS is planned for launch in 2019 to the solar-synchronous 700 km high circular orbit. The main goal of this mission is to study TGFs and TLEs in a wide wavelength range from radio to gamma (Blanc et al. (2007)). The main instrument of TARANIS is XGRE designed to detect TGFs and accompanied electron beams, so-called TEBs (Sarria et al. (2017)). XGRE consists of three scintillating detectors using $LaBr_3(Ce)$, with different observation

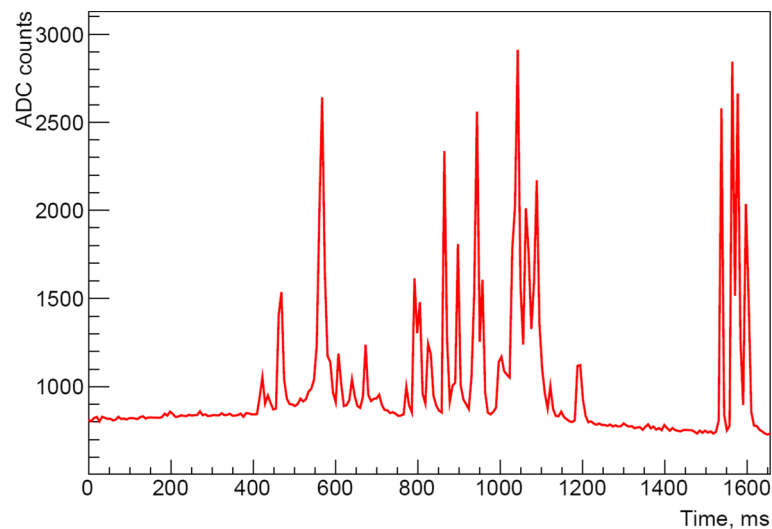


Fig. 4 Waveforms of a pixel brightness for an event detected at 03:23:27 UTC, January 4, 2017 above South America. Sampling time is equal to 6.6 ms

axis. Simultaneous observations of TGFs in gamma, optical, and radio bands are the main advantage of the TARANIS project (Farges et al. (2017)). For this purpose, the payload will include small aperture optical cameras, which provide TLE imaging in two spectral ranges of 757–767 and 772–782 nm that helps separate typical lightning and sprite effectively. Apart from two cameras, the TARANIS payload includes photometers for TLE timing in four wavelength bands of 170–260 nm, 332–342 nm, 757–767 nm, and 600–900 nm. Photometers have the same FOVs as optical cameras, and are able to produce trigger for all instruments on board. Payload also will include wide band radio frequency analyzer for electromagnetic signal waveform measurements in the frequency range from few kilohertz up to 37 MHz. Besides of the thunderstorm and lightning events identification, this instrument will be used also to study electromagnetic disturbances caused by electron precipitation, as well, as for the study of electromagnetic wave propagation in the ionosphere, and of the near-Earth space and of electromagnetic environment monitoring.

The ASIM (Atmosphere-Space Interactions Monitor) project (Neubert et al. (2006)) was launched on April 2, 2018 for the deployment on-board of the International Space Station (ISS), and on April 13 it was docked to COLUMBUS module of the ISS. It was developed for studies of the thunderstorm phenomena, of their possible influence on the upper atmosphere, and, especially, for the extensive study of TLEs and TGFs. The payload of ASIM includes X- and gamma-ray instrument MXGS and the optical instrument MMIA. The MXGS instrument (Budtz-Jørgensen et al. (2009)) consists of imaging X-ray telescope for the energy range of 10–400 keV, with the position-sensitive detector (PSD) as 128×128 matrix. A gamma-ray detector for the energy range of 0.2–40 MeV was also considered for use. X-ray telescope provides an angular resolution better than 1° in the mode of orientation to a point-like source. The optical instruments (MMIA) consist of the nadir-looking two cameras and three photometers.

The multi-pixel (1024×1024) CCD matrices are used as detectors in optical cameras, providing the spatial resolution about 300–400 m on the ground for the 400 km ISS typical orbital altitude. Photometer sampling rate of ~ 100 kHz provides the time resolution about $10 \mu\text{s}$. The MXGS instrument is planned to be operated continuously, except during the South Atlantic Anomaly (SAA) passage, and the MMIA should be operated only at the night side of the ISS orbit. Along with data recording in a monitor mode, the detailed data records should be made by triggers produced by both instruments. The generation of cross-trigger of payload complex is also foreseen. The instrument input windows are directed to the local nadir and toward the Earth limb.

The main goal of TRYAD (Terrestrial RaYs Analysis and Detection) experiment is multi-point observations in order to verify TGF beam models. The experiment is based on two identical 6U cubsats which in-orbit separation controls via aerodynamic differential drag. It is equipped with plastic scintillator coupled with silicon photomultiplier (SiPM). The crucial parameter of the experiment is an acquisition time accuracy which is provided by embedded GPS module.

The specific problems of TGF study

The problem of TGF origin is of specific interest. Discussing the future research on TGFs is necessary to note that the physical nature of their sources is not completely understood. The main unsolved problem with the TGF origin is the putative connection of TGFs with electromagnetic discharges of thunderstorms, and with TLEs. The solution of this problem is usually connected to the necessity of complex observations in the multi-frequency range of electromagnetic emission, from radio (tens of kHz) to gamma-rays (tens of MeV). It is expected that X-ray and gamma-ray instruments will provide localization of TGF source with the accuracy of a few degrees. For this purpose, it seems optimal to use combination of the wide-field detectors that will provide photometry with the high sensitivity, and of the Compton, or coded mask telescopes with the PSD, that will allow localization of the detected signal source. Detection of X-rays gives information about altitude of TGF source, because the X-ray intensity depends on matter thickness above the generation point. Identification of TGF source with given thunderstorm area or even with lightning requires the on-board simultaneous registration of event in radio, optics, and gamma. Coordinated observations with ground lightning observation networks, such as WWLLN and Vaisala are also necessary. For this purpose, the accurate (no less than $\sim 1 \mu\text{s}$) binding of detected event to the universal time (UT) should be provided by the satellite board.

In order to compare favorably with discussed above very impressive instruments of TARANIS and ASIM missions, it makes sense to expand the energy range, in which position resolution is possible, up to 1 MeV, or even more, taking into account hard energy spectrum of the gamma radiation from TGFs. It will be advantageous to combine the good space resolution capability with the possibility of high-resolution spectroscopic measurements in the range of up to ~ 10 MeV that will permit observations of TGFs in the gamma-ray nuclear lines. Taking into account, that TGFs are very short and the time resolution of the instrument under development has to be better than $\sim 10 \mu\text{s}$. The complex pixelated detector, composed of a large number of small independent sensitive elements, has much smaller chances for pile-up effects, than the large single crystal detector. It is also desirable to have capability

to detect electrons by the same instrument, which could be achieved by using X- and gamma-ray detectors for detection of electron bremsstrahlung.

The other approach, which could provide localization of TGF's source, is based on the use of triangulation technique for observations of the selected thunderstorm area from different satellites. Such method is very successful for cosmic gamma-ray burst (GRB) localization. In the case of TGFs it needs at least three satellites, which should be spaced at a distance of several hundred kilometers for orbits with altitude about 400–600 km. In this case, the GPS time accuracy will be enough for determination of time delay of TGF signals detected by different satellites, which gives thunderstorm area localization in limits of tens of kilometers. The separate problem is necessary to prevent the spread of satellites on distances more than abovementioned several hundred kilometers to provide simultaneous observations of given area from all satellites.

According to (Babich and Roussel-Dupré 2007), a photo-nuclear reaction, $^{14}\text{N}(\gamma, n)^{13}\text{N}$, may occur at TGF source or in surrounding matter because gamma-rays with energies above threshold of 10.5 MeV have been actually observed. Thus, photonuclear neutrons may be the clue to solve the problem of non-thermal mechanism in thunderstorm activity. Neutron production in TGFs was studied by (Carlson et al. 2010), who predicted that TGF produces $\sim 10^{12}$ neutrons at an average, that corresponds to a ground-level neutron fluence of $(0.03 - 1) \times 10^4 \text{ m}^{-2}$. Similar predictions were made by (Babich et al. 2010), who obtained neutron fluence of $10^3 - 10^7 \text{ m}^{-2}$ at ground level from gamma rays produced under the RREA mechanism. According to (Babich et al. 2010) a yield rate of a photonuclear neutron per one gamma quantum with energy over 10 MeV is 4.3×10^{-3} . An attenuation length of 20 MeV neutrons in the atmosphere was calculated as $\lambda_n = 13 \text{ g cm}^{-2}$ with the use of cross section of elastic and/or inelastic collisions with air nuclei (Shibata 1994).

The simulation of neutrons generated by gamma quanta during their propagation in the atmosphere was made also by (Drozdov et al. 2010) and (Grigoriev et al. 2010). They simulated the albedo neutron background and thunderstorm-produced neutrons, and then compared albedo and thunderstorm neutrons spectral parameters to estimate possibility of thunderstorm neutron detection in orbits with different altitudes up to 450 km. The energy spectrum of thunderstorm neutrons spreads from $\sim 1 \text{ keV}$ to $\sim 10 \text{ MeV}$, with a maximal flux at $\sim 6 \text{ MeV}$. Due to the scattering in the atmosphere, the main part of neutrons reaches orbital altitude from the point of origin in about several dozen of milliseconds. The maximal value of thunderstorm neutron integral flux will be observed in the time interval of 10 to 20 ms after the TGF, with the flux level up to $1.6 \text{ cm}^{-2} \text{ s}^{-1}$.

In view of the recently published results on the photo-nuclear processes and neutron generation during thunderstorms (Enoto et al. (2017)), the possibility of neutron detection in the range from $\sim 1 \text{ MeV}$ up to $\sim 20 \text{ MeV}$ will be also useful to have a direct indication of photo nuclear reactions in the TGF source. Thus, it is an independent channel, which allows estimation of hard energy photon number in the source. The other way is that neutron flux gives the estimation of accumulation of long-lived radionuclides in the atmosphere if they can be produced also in the gamma quantum interaction with the nuclei in the atmosphere.

All above considerations should be taken into account when choosing future advanced instruments for the TGF study. The present state of the field calls for the development of a new generation of gamma-ray imager/spectrometer with high resolution and sensitivity. Such instrument should be added by neutron detector or should be sensitive to the neutrons. It opens the way not only to multi-wavelength but also to a kind of multi-messenger observations.

Concept of TLE and TGF observations in the Universat-SOCRAT project

The next step in TAE study could be connected with Universat-SOCRAT space project of Lomonosov Moscow State University (MSU). It is a multi-satellite project for real-time monitoring in the near-Earth space of potentially dangerous hazards, that means the radiation environment; dangerous objects of the natural (asteroids, meteors) and of technogenic origin (space debris), as well as electromagnetic transients, i.e., cosmic gamma-ray bursts, optical, ultraviolet, and gamma-ray flashes originating in the Earth's atmosphere. Study of TGFs and TLEs is one of the high priority goals of this project.

Within the framework of the Universat-SOCRAT project, a few small satellites should be placed into specially selected orbits. For the minimal version, the group of satellites could consist of three satellites (Panasyuk et al. 2015). One spacecraft of medium mass (small satellite) should be launched on a low solar-synchronous orbit with an altitude of about 500–650 km and an inclination of $97^\circ - 98^\circ$. Two other satellites of lower mass (micro satellites) should be launched on an orbit close to circular with an altitude of about 1400–1500 km and an inclination of $\sim 80^\circ$ and on an elliptical orbit with an apogee of about 8000 km, a perigee of about 600–700 km, and an inclination of 63.4° . The mutual arrangement of the orbits is shown in Fig. 5.

The small satellite payload should include (Panasyuk et al. 2017) instruments for monitoring the space radiation, a set of instruments for optical monitoring of hazardous objects, a set of instruments to study atmospheric phenomena in the optical range, a set of instruments for

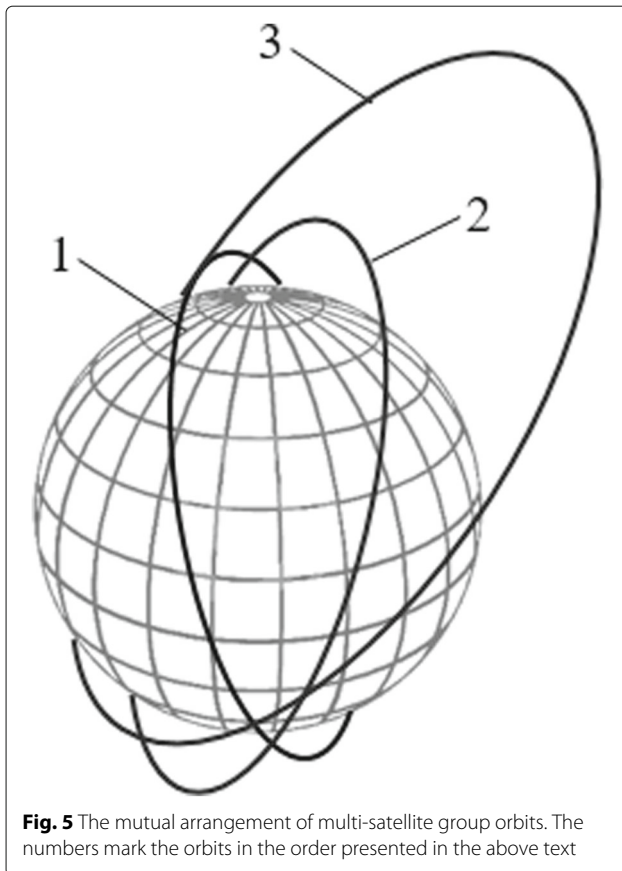


Fig. 5 The mutual arrangement of multi-satellite group orbits. The numbers mark the orbits in the order presented in the above text

monitoring in the gamma-ray range, and a special unit for data collection. The payload should also include three-component magnetometer. The payload of each micro satellite should include instruments for space radiation monitoring, a compact gamma spectrometer, a wide field-of-view optical camera, an ultraviolet detector, and an electronics unit for data collection.

Study of TLEs and TGFs will be realized mainly on the low orbital small satellite. Its polar orbit is not optimal for observations in gamma rays due to variable background. However, it provides a good opportunity to observe the different parts of the Earth's atmosphere including both equatorial and polar regions that significantly expands the possibilities of experiment in search of new kinds of TAE-like phenomena. On the other hand, the background conditions near the equator are quite acceptable for TLE and TGF study. The main scientific objectives from this point are multi-wavelength and multi-messenger observations. The first means the complex study of TGFs and TLEs in wide bands from red optics to gamma. The multi-messenger observations mean detection of high-energy electrons and neutrons simultaneously with optical, UV, X-ray, and gamma photons. The direct electron detection from thunderstorm

electron, gamma-ray avalanche, gives the direct confirmation of the theory of runaway electron breakdown and may confirm the mechanism of high-altitude discharges initiated by strong electric fields in the thunderstorm atmosphere. The neutron detection is necessary for estimations of hard photon number in TGF source as well as for accumulation of long-lived radionuclides in the atmosphere.

Experimental methods of TLE and TGF observations on the main satellite of the Universat-SOCRAT multi-satellite group

Instruments for TLE studies

The early MSU satellites provided a large amount of information on the properties of UV transient emission from the Earth's atmosphere, but at the same time they put forward a list of new puzzles that can be solved only by a new type of space-based telescope with spectrometric capabilities. Let us summarize these new problems that need to be studied, as well as the parameters of the detector needed to accomplish the task.

- 1 Long series of flashes have been detected. These series can be up to 10 min duration that corresponds to the distance of 4–5000 km along the satellite track. Series occur mostly above the regions of lightning activity but can continue even when the satellite leaves thunderstorm area. These flashes have various nature, but they point to a large-scale atmospheric activity.
- 2 Complicated temporal structure of UV flashes is observed at different time scales (from microseconds to seconds). But only short and separate time intervals were detected. Further studies with detectors having high spatial resolution are needed for better understanding of inter-relations of these events, as well, as continuous measurements with high-temporal resolution.
- 3 More detailed spectral information is needed to classify observed transients, understand their origin, and estimate more precisely altitude of their generation and development.
- 4 Energy distribution of the UV flashes detected in the previous experiments was calculated in the assumption of the nadir direction to the event. Absence of spatial resolution does not allow more accurate measurements of UV-flash energy. We note that good spatial resolution in addition to temporal and spectral resolutions of the used detectors is very important.

As a result of the considerations discussed above, a new detector mini-lens telescope—spectrometer) was developed for the Universat-SOCRAT project based on the

previous experience in UV detectors manufacturing at SINP MSU. This detector is aimed for monitoring measurements of transient atmospheric events with a high ($\sim 1 \mu\text{s}$) temporal resolution in a number of wavelength bands. MLT-S will provide imaging of the events, energy distribution in the spectrum of optical radiation (from near UV to NIR), and temporal profile of the signal.

The detector consists of three main parts:

- 1 Telescope;
- 2 Spectrometer;
- 3 Data processing system.

The 3D model of the detector is shown in Fig. 6. Dimensions of the detector are $20 \times 20 \times 30$ cm, total power consumption does not exceed 10 W and mass of the detector is near 7.2 kg. The most massive part is an aluminum box, so the weight of the flight model of the MLT-S can be significantly decreased by using carbon-plastic materials in the mechanical structure. Entrance windows of the telescope and spectrometer are in the nadir direction and equipped with black blends which protect the detector from the side illumination.

The MLT-S telescope is based on the experience of mini-EUSO development (Capel et al. 2018) and represents a detector with a simplest optical system composed of one lens of 5 cm diameter and a photodetector. The lens has a spherical front side (radius of curvature is equal to 82.32 mm) and plane rare side. This lens provides 50 times more sensitivity than detectors on satellites Tatiana and Vernov (UV flashes with number of photons released in the atmosphere $\sim 10^{15}$ can be measured).

The photodetector is one elementary cell (EC) of the mini-EUSO detector and consists of four multi-anode

photomultiplier tubes (MAPMTs) which are placed in a focal plane of the lens. Total amount of pixels on the focal surface is 256 which compose a matrix 16×16 . EC has one Cockcroft-Walton high-voltage (HV) power supply, which provides HV for all MAPMTs and is controlled by the data processing system in order to change the gain of the MAPMTs for the cases of high brightness of the event or high level of UV background.

Each pixel of MAPMT has ~ 3 mm size, and focal length of the optical system is 15 cm. For this configuration, the telescope resolution is 1.2° , which provides a spatial resolution on the Earth's surface ~ 10 km for 500 km altitude of the satellite orbit. These parameters lead to observed area of $25,600 \text{ km}^2$ in the atmosphere. The optical scheme and ray tracing for $0^\circ, 4^\circ, 8^\circ, 9^\circ$ zenith angles are shown in Fig. 7.

The MAPMT is operated in the single-photoelectron mode and provides high sensitivity of the detector. This mode is performed by using an application-specific integrated circuit (ASIC) of the SPACIROC-3 (Spatial Photomultiplier Array Counting and Integrating Read Out Chip) type, which was developed earlier for the JEM-EUSO experiment (Blin-Bondil et al. (2014)). Photons are counted by SPACIROC-3 for 1 or $2.5 \mu\text{s}$ time bins that correspond to temporal resolution of the detector.

Spectrometer is made of 16 single-anode PMTs Hamamatsu R1463 which were used in the TUS experiment (Klimov et al. (2017)) on-board the Lomonosov satellite (Sadovnichii et al. (2017)). These PMTs compose a matrix 4×4 and each PMT has an individual filter on the entrance window. It means that each PMT measures the radiation from the whole FOV, but in a specified wavelength range.

We hope that measurement of the transients spectrum will allow us to determine the type and altitude of the

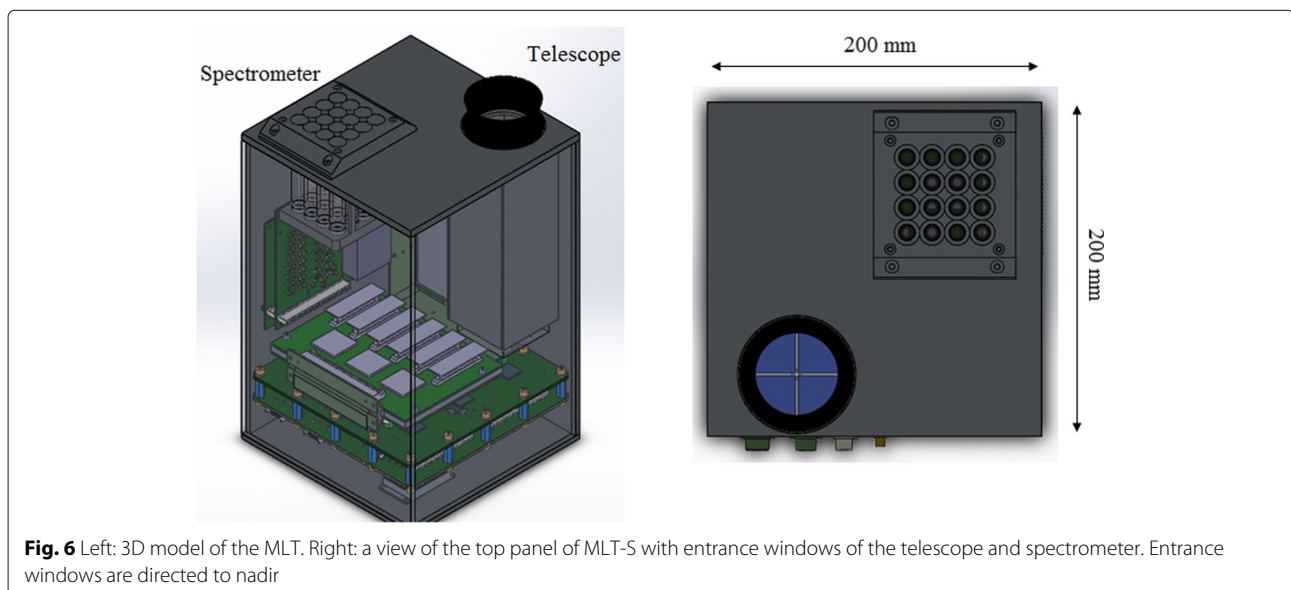
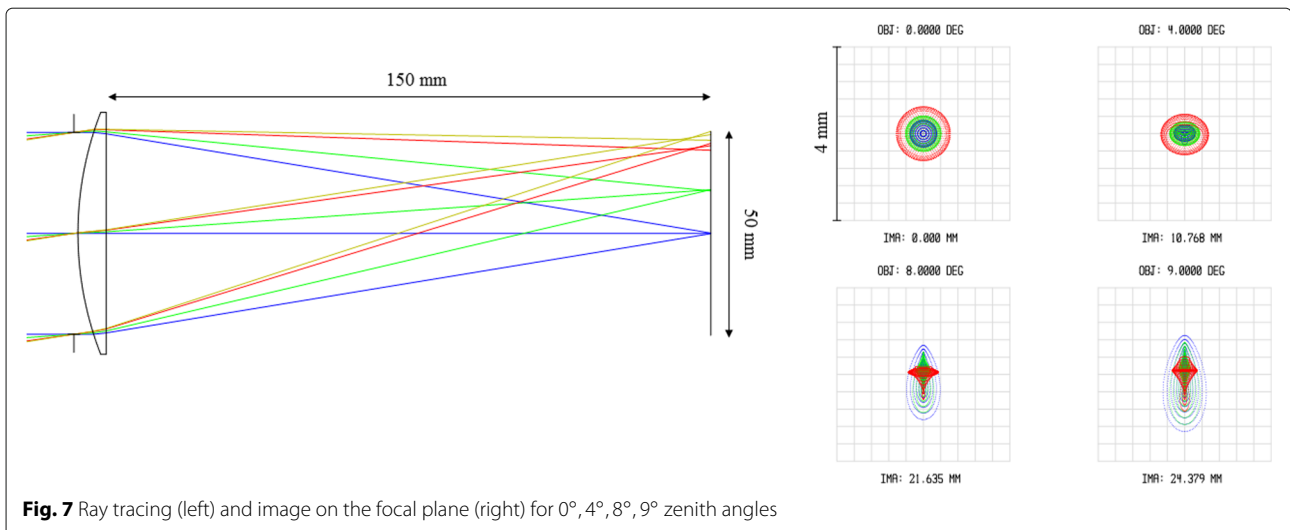


Fig. 6 Left: 3D model of the MLT. Right: a view of the top panel of MLT-S with entrance windows of the telescope and spectrometer. Entrance windows are directed to nadir



event. UV and NIR filters will be used to have a possibility to compare new results with that of the previous MSU experiments (Tatiana-1, Tatiana-2, and Vernov), where UFS1 (240–400 nm) and KS11 (600–800 nm) filters were used. This will allow us to make preliminary estimates of the event height using the old method, suggested by (Garipov et al. 2013) and applied to Tatiana-2 data.

We plan to use the atomic oxygen absorption line (762 nm) additionally in order to separate low-altitude events from the high-altitude atmospheric luminous phenomena. The chosen oxygen absorption line should be faint for lightning discharges occurring deep in the atmosphere. The same spectral bands were used by spectrophotometers on-board ISUAL (Chern et al. (2003)) and JEM-GLIMS (Ushio et al. (2011)). On the other hand, one of the most intense lines in the lightning spectrum at 777 nm (Orville and Henderson 1984; Sharkov et al. 2018) will be used for detection of lightning events. Other spectral bands can be selected for various purposes, like to derive an altitude of the event or mean energy of electrons in the discharge, etc. All spectral bands suggested for use in the spectrometer are summarized in Table 1.

In comparison with already performed missions (ISUAL, JEM-GLIMS) and other planned missions, like ASIM and TARANIS, a number of spectrophotometers in a new MSU spectrometer is enlarged to 16, comparing to previously used 4 or 6, and the selected temporal resolution is much better, i.e., $\sim 1 \mu\text{s}$ vs $50 \mu\text{s}$ of JEM-GLIMS, for example. This fact will allow measurements of the temporal and spectral structure of the atmospheric events in much more details, as well as to achieve a reliable separation of various types of atmospheric phenomena.

Data processing system of the spectrometer will be based on a Xilinx Zynq XC7Z030 system on chip. This chip includes both a high-speed logic part (a field programmable gate array—FPGA) and a processor

Table 1 Spectrometer wavelength bands

#	Wavelength (nm)	Comment
1.	240–400	UFS1, UFS2, KS11 filters for comparison with MSU experiments (Tatiana-1, Tatiana-2, and Vernov)
2.	270–380	
3.	> 600	
4.	762.7	TLE marker—atomic oxygen absorption line
5.	777.4	Lightning marker—the brightest line in lightning spectrum, used for lightning detection in LIS (Orville and Henderson 1984) and convergence ((Sharkov et al. 2018)) experiments
6.	500.1	Lightning marker—bright line in lightning spectrum and absent in sprite spectrum ((Milikh et al. 1998))
7.	337	$\text{N}_2^+ 2\text{P}$ line—marker of low latitude and should absent in lightning spectrum due to ISUAL data
8.	391.4	$\text{N}_2^+ 1\text{N}$ —line of ionized atomic nitrogen
9.	427.8	$\text{N}_2^+ 1\text{N}$ present in aurora light and marker of ionization source (energetic charge particle flow)
10.	470.9	
11.	690	Meinel band—marker of high latitude and high energy of electrons involved into the process
12.	388.3	Cyanogen (CN) emission, a spectral signature of lightning flashes with continuing current (monitoring of lightning that can cause forest fires ((Christian et al. 1983; Fuquay et al. 1967)).
13.	294	Signature of extremely high altitude event (lines of $\text{N}_2(\text{VK})$ system)
14.	313	
15.	399.8	$\text{N}_2^+ 2\text{P}(1,4)$ analyzed by (Armstrong et al. 2000), in comparison to 427.8 nm and 470.9 nm lines
16.	Without filter	Total emission of lightning or TLE measurements

system. It allows development of a high-speed data-processing system and implementation of different triggering algorithms. Using of 1 Gb DDR memory provides continuous writing of information with high frequency directly from the FPGA part via high-speed Ethernet interface to the board computer to store all this information.

The whole system can operate in different modes with different triggers. The first mode is a continuous monitoring of the atmospheric emission with high temporal resolution of $2.5 \mu\text{s}$. This mode allows measurements of UV emission along the satellite track almost without dead time, and thus will provide information on the transient temporal structure with high resolution. It is necessary in order to understand the series of flashes detected in previous MSU experiments. This mode will produce a huge amount of data; therefore, only a few channels of the spectrometer will be used during these measurements and on the selected part of the orbit. Slow monitoring mode with temporal resolution of $\sim 1 \text{ ms}$ (similar to one used during the Tatiana and the Vernov experiments) is selected as the second mode. This mode produces three orders of magnitude less information in comparison to the first one, and thus will allow simultaneous measurements by telescope and spectrometer. This mode will give us information on spatial structure of events in series. The third mode of spectrometer is a variety of triggering regimes, like (1) several threshold triggers of spectrometer with various temporal resolutions, $2.5 \mu\text{s}$, 0.2 ms , and 3 ms , which select events exceeding a threshold in a definite spectrometer channel, and (2) a number of telescope triggers in which a spatial structure of the events is analyzed in addition to amplitude. It will allow selection of the events with a specific geometry (such as elves, for example, where a ring structure is expected, or, alternatively, a linear track of meteors).

In addition to MLT-S, the satellite will be equipped with a modified detector DUV similar to the detector used in the Vernov and Tatiana missions, but with an additional far UV channel (100–300 nm). This wavelength range is very useful for selection of high altitude events, because the emission from low altitude lightning in this? range is efficiently absorbed by the ozone layer. This way of TLE selection is partially used in the JEM-GLIMS spectrometer (Sato et al. (2017)).

TGF observations in the Universat-SOCRAT project

Instruments for TGF study of the Universat-SOCRAT project will include gamma-ray flash monitor (GFM), and a tracking gamma-ray spectrometer (TGS) of the high resolution and sensitivity, that will be sensitive also to neutrons with energies from about 1 MeV up to several dozen of megaelectron volt. The separate unit for data analysis and control of GFM and TGS should be also foreseen in

the payload. This unit should contain digital electronics unit that will provide the record of data stream with a time resolution of $\sim 10 \mu\text{s}$, and generate the triggers enabling the detection of different type of events, including TGFs and neutron flux increases. The data record must be referenced to the UTC time with an accuracy of $\sim 1 \mu\text{s}$ to allow the positioning of the TGFs, if observed simultaneously by several space missions, using triangulation, and for the comparison with the data of ground based lightning location networks. Both instruments, TGS and GFM, should be installed on the medium mass satellite similar to that used for Vernov mission. It provides the payload mass about 100 kg that is enough for these instruments.

Tracking gamma-ray spectrometer

Tracking gamma spectrometer of high resolution and sensitivity is a combination of two space (position) sensitive units, so-called hodoscopic and calorimetric. Both units should be connected in a mono-block construction (see Fig. 8). The coded mask, with a random pattern coding aperture, will be placed above the calorimeter unit at a distance of $\sim 50 \text{ cm}$. The instrument axis should be directed along the nadir—zenith axis—in such a way that the instrument should be directed to the local nadir from the hodoscope side, which should be used mainly for detection of neutrons from the atmosphere. In the case of TGF detection, such orientation allows estimation of detected quanta inclination angle using scattering parameters of those quanta that will deposit some part of their energy in at least two points of hodoscopic and calorimetric parts of the instrument. It also will allow effective separation of gamma quanta from neutrons and charged particles. Absorption of gamma quanta in the calorimetric unit also allows determination of their energy.

The combination of hodoscopic and calorimetric units assumes operation of the instrument in the mode of the dual Compton scattering. It permits to check the appearance of the GRB from the Earth's atmosphere and to separate real gamma-ray events as TGFs from the cases of electron precipitation. Image reconstruction using the coding mask telescope will allow localizing the GRB source and thus will help to separate GRBs from TGFs. The multi-pixel detectors used both in hodoscopic and in calorimetric units permit to eliminate significantly the contribution of pile-up pulses that is very important for detection of very fast events such as TGFs. The detection of false bursts imitated by cosmic ray energetic particles can be completely excluded with the use of multiple coincidences.

The instrument apart detectors will contain the data processing unit based on digital electronics that allows for very fast data recording with sufficiently high time resolution of $\sim 1 \mu\text{s}$. It also should provide the on-board analysis of images obtained from the coding mask telescope and

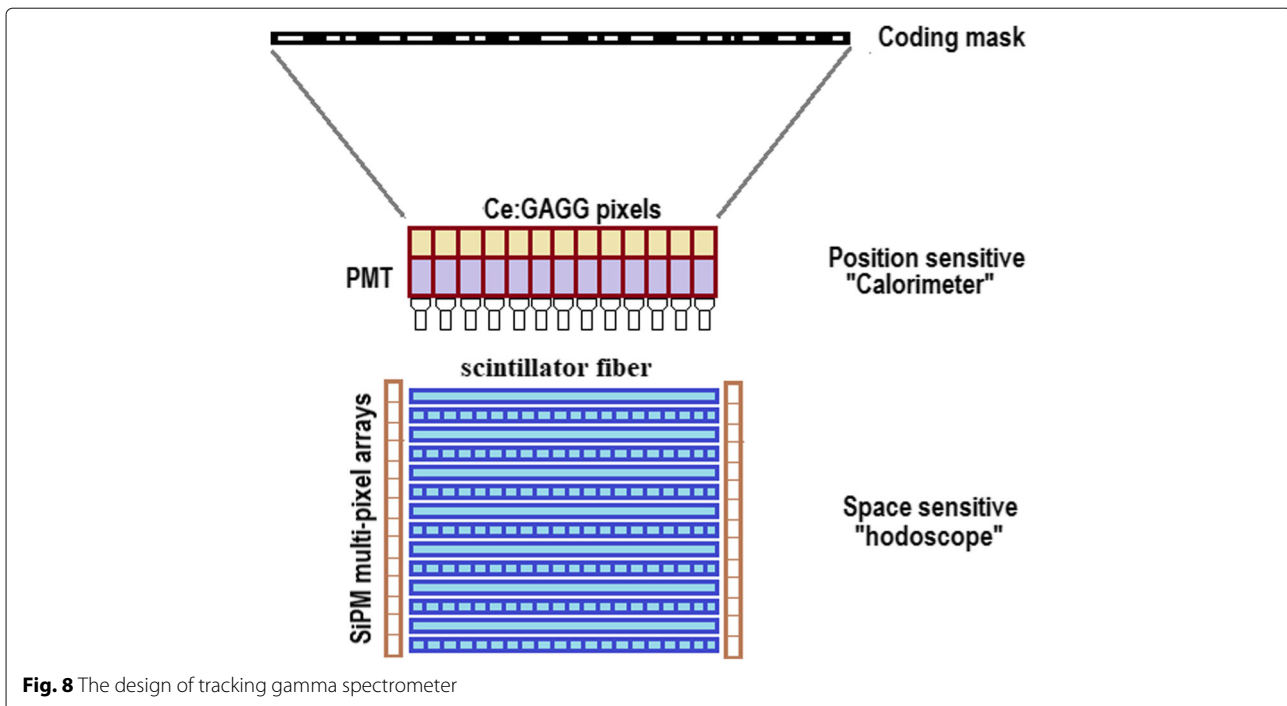


Fig. 8 The design of tracking gamma spectrometer

from the system of hodoscope—calorimeter—operated in the double Compton scattering mode, as well, as to generate the GRB and TGF triggers.

PSD in hodoscopic and calorimetric units allows localization of the place of particle or quantum interaction in the detector. It makes possible to obtain information about space distribution of detected fluxes. To the present, the main directions of PSD development for gamma-ray astronomy are connected to improving the PSD detection efficiency, to lower the detection threshold, to increase the accuracy of the source localization, to reduce the distorting effect of the “dead time” of the detector, and to improve the time resolution.

The both calorimetric and hodoscopic units of the instrument should be consisted of a number of identical modules, providing possibility for increasing of the effective area and thickness of the detector, depending on the overall mass resources of spacecraft. Then, we will consider the instrument parameters for calorimetric and hodoscopic units in a minimally reasonable configuration.

Thus, the hodoscopic unit of tracking gamma spectrometer should be a set of light-conducting scintillation fibers of small thickness (0.15 cm or smaller), located in layers in such a way that in adjacent layers, the orientation of the fibers is normal to each other (see Fig. 8). This system allows separation of events connected to the detection of gamma quanta and neutrons. The principle of detecting gamma quanta is determined by their Compton interactions in fibers, and the detection of fast neutrons occurs in the mode of their elastic scattering by hydrogen nuclei

in the scintillation fiber (Iyudin et al. 2015). The low-fiber thickness provides a high-spatial resolution when gamma quanta and neutrons will be detected, as well as a low threshold for the detected photon under the condition that the energy must be released in the interaction act at least in two neighboring layers. The multi-pixel matrices of SiPMs will be used as photosensors for recording light flashes in fibers. The matrix photosensitive surfaces should be facing the ends of fibers, positioned in such a way that each fiber is viewed by the corresponding cells (“pixels”) of two photosensors (SiPMs).

We are currently planning to use 12×12 quadratic matrices of SiPMs, with a 3×3 mm cell size of SenSL production. The dimensions of one matrix are $48 \times 47 \times 10$ mm³, and its mass is 26 g. Thus, for the minimal configuration with a hodoscope size of $150 \times 150 \times 150$ mm³, it is necessary to use 36 SiPM matrices of 12×12 dimension to read-out light pulses from the hodoscope.

An advantage of this instrument is the possibility of implementing different triggers. One of them will allow selection of the events corresponding to the elastic scattering of fast neutrons with energies from 5 to 100 MeV, based on the kinematics of the scattering event itself in the presence of two (or more) neutron interaction points in the volume of the hodoscope. While under conditions of an increased background of charged particles, it is possible to use a trigger where outer layers of the hodoscope are used for the purpose of protecting the internal part of the instrument from the charged particle penetration into it. Thus, the anti-coincidence shield is realized. The trigger

condition can be checked by the digital unit according to the given algorithm, and it is possible to correct the algorithm, depending on the specific background conditions and the choice of the most priority tasks.

The calorimetric unit will consist of a set of minimum 1616 scintillating crystals of Ce:GAGG type, with size of $1.0 \times 1.0 \times 3.0 \text{ cm}^3$ each, that should be placed on the top of the instrument. In the case of detection of TGE, calorimetric unit will detect gamma quanta scattered in the hodoscope. Ce:GAGG crystals have quite high light output ($\sim 57000 \text{ phot/MeV}$) and density ($\sim 6.7 \text{ g/cm}^3$) with sufficiently small decay time of $\sim 80 \text{ ns}$ (Iwanowska et al. (2013)), that ensures a high throughput of the unit. The fast crystals help to realize the high accuracy of the time measurements and high throughput of the measuring channel. Relatively high density of Ce:GAGG crystals provides the high efficiency of gamma quantum detection in wide energy range. Due to the high light output Ce:GAGG scintillators also give good energy resolution. For example, we have tried Ce:GAGG pixels with thickness of 3.0 cm and found the high-detection efficiency of gamma quanta with energies up to a several MeV, and an energy resolution of $\sim 4\%$ at 1 MeV.

The SiPM light sensors or small vacuum photomultipliers could be used for viewing of Ce:GAGG crystals. For example, Hamamatsu R1463 is quite compact photomultiplier with a diameter of input window of 13 mm. R1463 photocathode is sensitive at the wavelengths of 300–650 nm, with maximum cathode sensitivity at about 420 nm, that is in good correspondence with the emission spectrum of Ce:GAGG.

The tracking gamma spectrometer has its own read-out unit of analogues and digital electronics.

The instrument parameters are given in the Table 2.

Experimental test of energy resolution of a one-pixel element of the calorimeter was done with a scintillating detector module based on the mirror-coated Ce:GAGG crystal with the size of $10 \times 10 \times 10 \text{ mm}^3$ attached to the PMT of Hamamatsu R1463 type. A standard set of radioactive gamma-ray sources including ^{137}Cs , ^{207}Bi , and ^{241}Am were used for module calibration. Experimental measurements of energy resolution are useful because several factors including non-uniformity of light collection in the detecting crystal influence on it.

The value of energy resolution was determined from the full width at the half maximum of the corresponding peak on the energy spectrum. The minimal and maximal energy of the range also were determined. The low energy threshold was $\sim 20 \text{ keV}$, and the upper limit for the measurements was $\sim 10 \text{ MeV}$. Low limit of the detector energy range is mostly determined by the absorption of soft gamma-rays in the substance of the instrument input window while the maximal value is determined by electronics. It was confirmed by the measurements that Ce:GAGG

Table 2 The tracking gamma spectrometer parameters

Parameter, units	Value
Energy range for gamma quanta, MeV	
All interactions	0.02 – 10.0
Coding mask telescope	0.02 – 1.0
Double Compton imaging	0.5 – 10.0
Effective area, cm^2 (all interactions)	~ 250
Angular resolution	
Coding mask telescope	$\sim 2^\circ$
Double Compton imaging (at 1 MeV)	10 – 15°
Time resolution, ns	5
Energy resolution (at 1 MeV)	5%
Sensitivity to the 1 ms burst detection, cm^{-2}	$3 \cdot 10^{-2}$
Energy range for neutrons, MeV	3 – 100
Effective area for neutrons, cm^2 (at 40 MeV)	13
Mass, kg	40
Information capacity, MB/day	~ 500
Power consumption, W	60

scintillator has stop-factor high enough for good resolution of 1.17 MeV and 1.33 MeV lines from ^{60}Co , even using quite small crystal with the size of $10 \times 10 \times 10 \text{ mm}^3$.

The energy resolution at 1.77 MeV (isotope ^{207}Bi) is 4.6%. The energy dependence of the resolution of the detector with Ce:GAGG can be approximated by inverse proportionality to the root of the energy so the main contribution to the energy resolution is due to fluctuations in the number of photo-electrons, and the expected effect of non-uniform light collection is not significant.

Measurements of the light absorption in the scintillation fiber were also made in order to test the possibility to use such fiber as an element of the hodoscope in correspondent energy range. The measurements were made for two kinds of fibers with square section and the size of 3 mm and 1.5 mm. In each measurement, several layers of fibers were placed into a special grid. The light-sensitive SiPM array was placed at the end face of the fibers. For the measurements, a collimated source of the ^{90}Sr decay electrons with a $\sim 5 \text{ mm}$ diameter beam was used. The source was placed above the fiber in such a way that the radiation spread along one column of the multi-pixel photodetector. The coincident events in at least two upper layers of fibers were selected, in order to guarantee that the energy release in the layer nearest to the source of electrons was $\sim 600 \text{ keV}$ for 3 mm fiber and $\sim 300 \text{ keV}$ for 1.5 mm fiber. The source moved along the fiber, the amplitude spectra were collected for each position, and the channel of the peak maximum for the collected amplitude spectrum was determined. The measurements show that 15 cm long fiber with 1.5 mm quadratic section absorbs

not more than 50% of the scintillation light trapped by the fiber. More light is collected when the light is collected from the both ends of the fiber that permits us to conclude that such fibers can be successfully used in the TGS hodoscope.

We have tested also the time resolution for different combinations of scintillating crystals and of photosensors. The test was done with the use of a coincidence method, using radioactive sources producing two gamma quanta at the same time. Isotope ^{22}Na emitting two annihilation gammas with energy 511 keV in opposite direction was selected, as well as ^{60}Co that decays producing two photons with energies of 1.17 MeV and 1.33 MeV, with the picosecond delay. The decay events with pulses produced in two detectors were used as a start and stop signals that were fed into the board of time-code converter P7889, by FAST ComTec company, providing the measurement of time delay spectra with 100 picosecond resolution. Collecting and processing of time delay spectra was done by special MCDWIN software provided with the measurement board. The tests were made for the PMT+Ce:GAGG modules as well as for the SiPM+scintillating fiber modules, and for their combination. The time resolution of less than 1 ns was obtained in all combinations. This good timing will allow analyzing of the events produced by the gammas and neutrons in TGS at the distances of ~ 10 cm.

Gamma-ray flash monitor

The GFM instrument should provide the monitor type observations of the upper atmosphere in the hard X-rays and soft gamma-rays, in an energy range of 0.01–3.0 MeV, with the possibility of rough localization of the TGF source. GFM will consist of three identical detector units, which are similar to the detector unit used as gamma-ray burst monitor of the Lomonosov mission (Svertilov et al. 2018). This detector is also the successor of detectors that successfully registered TGF on the Vernov satellite (Bogomolov et al. (2017)).

The axes of GFM detectors should be oriented at 90° relative to each other, similar to the mutually normal edges of the cube, thus forming a Cartesian coordinate system. With this configuration, the main diagonal of the cube will be directed to the local nadir. The possible location of GFM instrument on the satellite payload panel is shown in Fig. 9. The sensitive area of each detector has a cosine angular dependence which within $\sim 60^\circ$ of its axis is not shadowed by any element of the spacecraft (see Fig. 9). This configuration will allow the rough estimation of TGF source location in the atmosphere by comparison of the amplitudes of the different detectors output signal, similar to the KONUS concept of the GRB source localization (Mazets and Golenetskii (1981)).

Each detector unit consists of a layer of thin (0.3 cm) NaI(Tl) crystals positioned above a considerably thicker (1.7 cm) layer of CsI(Tl) crystals (see Fig. 10). The diameter of each of these scintillators is 13 cm. The NaI(Tl) is placed on top of the CsI(Tl) crystal and optically coupled with it. Both scintillator layers are viewed simultaneously by a single Hamamatsu R877 PMT. The thickness of the NaI(Tl) layer is optimized to detect the soft photons. Energy ranges are 0.01–0.5 MeV for the NaI(Tl) crystal and 0.05–3 MeV for the CsI(Tl) crystal. In this configuration, the NaI(Tl) layer serves as the main detector for hard X-ray timing, while the CsI(Tl) crystal is used as an active shield against background gammas, but it can be used also to detect gammas with energies up to few MeV.

The GFM detector units' parameters are given in the Table 3.

The difference of decay times for the NaI(Tl) ($\sim 0.25 \mu\text{s}$) and CsI(Tl) ($\sim 2.0 \mu\text{s}$) crystals provides an opportunity to separate light flashes in these crystals by the pulse shapes with the help of special electronics. A PMT signal with negative polarity is characterized by fast increase in amplitude that is followed by a slower exponential decay. The signals from a set of crystals integrated during the first ~ 800 ns after trigger are called "fast" component, during the following $\sim 3 \mu\text{s}$ —the slow component. The ratio of fast to slow components will allow separation of the cases of energy deposition in different parts of the detector. It is necessary to note that due to sufficiently long decay time of CsI(Tl) crystal, the so-called pile-up effect can be significant in $\text{NaI(Tl)}/\text{CsI(Tl)}$ phoswich detectors. The BDRG Lomonosov experience indicates on that pile-up effect is real at high counting rates. The only way to avoid pile-up is using of more fast scintillators. Thus, for example, possibility of using of $\text{LaBr}_3(\text{Ce})$ or CeBr_3 and BGO combination except $\text{NaI(Tl)}/\text{CsI(Tl)}$ should be considered.

Detector response matrix was simulated with the use of MEGAlib toolkit v.2.29.01, which utilizes the GEANT4 databases (geant4-10-00-patch-03 (Zoglauer 2005; Zoglauer et al. 2006)). Several dozen of simulation sessions of gamma quantum and electron parallel beam interactions with the GFM detectors were made for various beam directions relative to the detector axis. These beam directions were characterized by zenith angle θ_1 (i.e., the angle between beam direction and detector axis) and the azimuth angle θ_2 (i.e., between the beam projection on the detector plane and the detector axis). In different sessions, the gamma-ray energy spectrum was chosen as a power law with the different power index values, and the band models were used also, with the different sets of E_c , α , β parameter values.

Our simulations determined the detector energy threshold to be about 20 keV at $\sim 20\%$ efficiency for NaI(Tl) . Radiation with the energy values between 10 and 20 keV

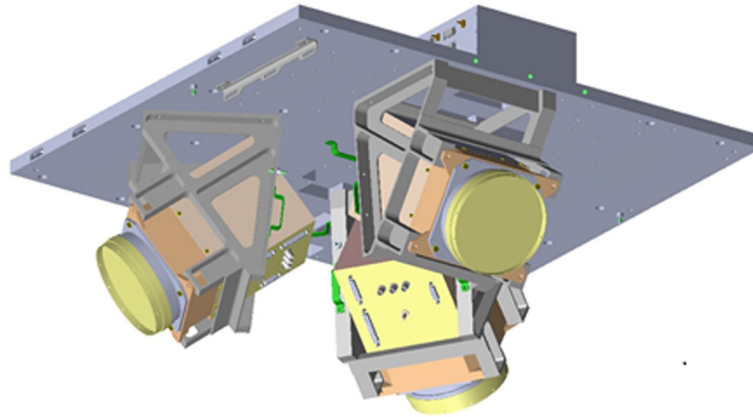


Fig. 9 The general view of the location of the GFM detector units

can be detected also but with the smaller efficiency of ~ 5 to 20%. Gamma-rays having energy more than 200 keV can pass through $NaI(Tl)$ layer and penetrate the $CsI(Tl)$ crystal. The efficiency of $CsI(Tl)$ detector at 1 MeV is about 30%. Similar calculations were made for the electron beams with power energy spectra. The obtained energy threshold for electrons was derived as ~ 300 keV for $NaI(Tl)$ and ~ 2 MeV for $CsI(Tl)$ crystals, respectively. Both values indicate the primary energy of electrons without energy losses in the instrument cover.

The phoswich method based on the combination of two-layer scintillator with different decay time such as $NaI(Tl)$ and $CsI(Tl)$ crystals viewed by a given PMT permits the effective separation of events in these scintillators. While observing certain burst-like count increase one can compare numbers of events with energy release in the $NaI(Tl)$ and $CsI(Tl)$ crystals. Gamma quanta with energies of about several hundred kiloelectron volts will interact both in $NaI(Tl)$ and $CsI(Tl)$ scintillators. In the case of electrons with similar primary energies, events with energy released only in $CsI(Tl)$ will be absent. This approach is sufficient for effective discrimination of the real gamma-bursts against the background of electron flux variations, including short, precipitation-like, increasing intensity phenomena.

The TGF source location can be estimated by comparing the output readings N_i of the three GFM detectors using the cosine function to adjust the beam coordinates. The axes of the detectors are shifted at 90° from each other so that the TGF source angle coordinates θ_1 , θ_2 , and θ_3 can be calculated from the simple formulas:

$$\cos\theta_1 = \frac{N}{\sqrt{N_1^2 + N_2^2 + N_3^2}},$$

$$\cos\theta_2 = \frac{N}{\sqrt{N_1^2 + N_2^2 + N_3^2}},$$

$$\cos\theta_3 = \frac{N}{\sqrt{N_1^2 + N_2^2 + N_3^2}}.$$

Used in the formula, N_i values can be estimated as excess counts in a given detector if one compares detected gamma quanta during flash with the expected number of background counts, extrapolated from this detector's readings immediately prior to the burst beginning. Obviously, the TGF source position accuracy depends on the TGF fluence and the background count rate at the time of

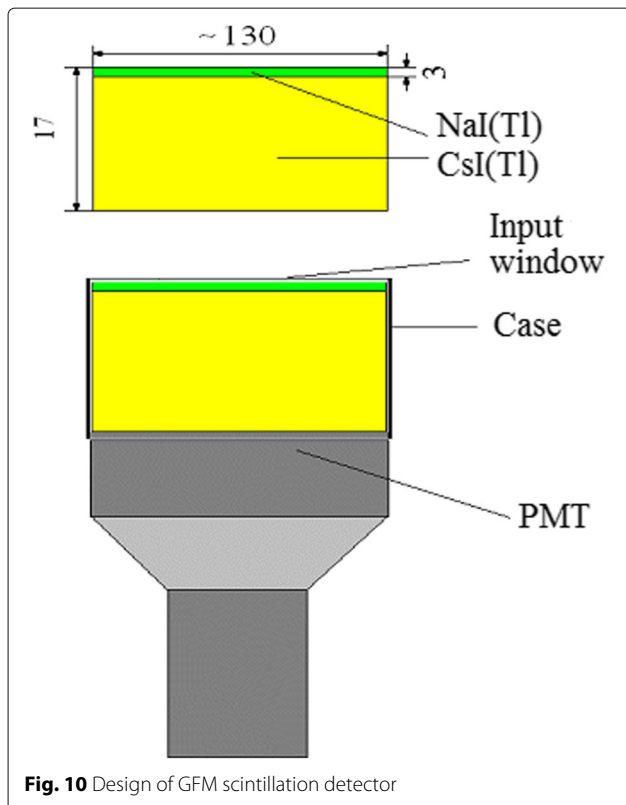


Fig. 10 Design of GFM scintillation detector

Table 3 GFM detector units' parameters

Parameter, units	Value
Energy range, MeV	0.01 – 3.0
Effective area (for three detectors), cm^2	~ 360
Time resolution, μs	1
Field of view, sr	2
Energy resolution (at 1 MeV)	5%
Sensitivity for 1 ms burst detection, cm^{-2}	$\sim 3 \cdot 10^{-2}$
Accuracy of burst source location	$\sim 10^\circ$ (for the brightest events)
Mass (for one detector module), kg	5.5
Information capacity, MByte/day	~ 500
Power consumption, W	22.5

trigger. The calibration accuracy of each detector determines the systematic component of the TGF source error box.

The TGF source location accuracy for the GFM instrument was estimated by numerical simulations. The TGF source position in the instrument FOV was chosen, then gamma quantum position and interaction parameters in the detectors were simulated for the given distributions of energy and duration. Then, the number of detected gamma quanta in each detector was determined for a given energy range. Using the detectors outputs the TGF source coordinates were derived. Such simulations were repeated many times for bursts with given energy spectrum, flux values, and durations. The root mean square (RMS) of the detection angles of the restored source and hence, its error box, were also determined.

In order to estimate the direction reconstruction error, a 1/6th portion of the whole GFM field of view, i.e., crossed area of three detector FOVs, was bombarded by gammas, and 79 arrival directions were distributed evenly across this area. Three GFM detectors were treated separately for each arrival direction because the incident gamma flux was observed by them from different aspect angles. For each detector, all events with non-zero energy contribution to the *NaI(Tl)* and/or *CsI(Tl)* crystals were recorded. In order to make direction error estimates statistically robust, 20 independent samples were simulated for each arrival direction with different values of spectral index and fluence (S).

The accuracy of TGF source localization depends on the brightness and hardness values of the TGF and the background level. The typical error box for very bright events with a fluence of ~ 1 phot/ cm^2 is expected to be $\sim 5^\circ$, while for weak flares (~ 0.1 phot/ cm^2), it may exceed 10° . For the expected satellite orbit altitude about 500–600 km, it corresponds source area accuracy ~ 40 and ~ 100 km, respectively. It is quite rough positioning; however, it permits to connect the detected TGF event with a nearby

thunderstorm area. More accurate TGF source location can be realized by using of position-sensitive tracking gamma ray spectrometer.

Discussion and results

Further progress in understanding of TLE and TGF phenomena can be achieved via the multi-wavelength and multi-messenger approach. The latter means the inclusion of hadronic signature of the phenomena in the process of understanding via the neutrons that are likely generated by high-altitude discharges, similar to the abovementioned neutron generation during thunderstorms (Enoto et al. (2017)).

Multi-wavelength observations of TLEs and TGFs will be realized with the use of above-presented combination of optical ultraviolet, X-, and gamma-ray instruments. For clear thunderstorm identification, radio-frequency analyzer at least for wavelength band from several dozen kilohertz up to 15–20 MHz should be added to the mission payload.

Taking into account the ranges of TGF, observed intensity and rate obtained by GRB Fermi (Tierney et al. (2013)), i.e., 0.05 – 0.5 count/ cm^2 /TGF and 10^{-7} – 10^{-9} TGF/h/ km^2 , respectively, we can estimate the expected sensitivity of TGS instrument for minimal configuration (256 cm^2) as ~ 10 counts per 1 TGF. Then, for polar orbit with ~ 500 km altitude and about $\pm 30^\circ$ instrument field of view, the expected number of events will be about 1 event per day from near equatorial areas. Thus, for the time of experiment of about 3–5 years, the significant statistics of TGFs could be obtained. The sensitivity and, thus, the expected TGF statistics for GFM instrument is quite similar.

However, the crucial point in understanding of TGFs physical nature is confirming or refuting their direct connection with the given thunderstorm or lightning. For this goal, besides of the event fine timing, a good localization of the TGF source is also necessary. Of course, the angular resolution presented above for both GFM and TGS instruments, even for intensive TGFs, is not better than $\sim 10^\circ$ that scales to the space accuracy of TGF source localization of ~ 100 km for the instruments flying at 500 km orbit. It is enough for TGF source identification with thunderstorm area, but it is insufficient to guarantee the identification with a given thunderstorm cloud. This latter task will demand an improvement of the angular resolution of suggested instruments by at least a factor of 10. The solution for the localization problem can be achieved by applying the triangulation method for observations of the selected area with different satellites. As it was mentioned above, for this purpose, the Universat-SOCRAT multi-satellite mission could be added by some number of CubeSats, which should be launched with the main spacecraft into similar orbit for the joint observations of a given

area. Sufficiently, light X-ray and gamma-ray detectors aimed for the TGF detection only, without spectrometer capabilities onboard the CubeSats will provide realization of the triangulation technique. By this, the necessity of maintaining of given distance between satellites is a separate technical problem. It can be solved using thrusters on micro-satellites.

The other result in TAE study could be connected to the possibilities of neutron detection. Simulation predicts detection of about two neutrons for event time 30 ms at the orbit with 450 km altitude, by the detector with 60 cm² effective area (Drozdov et al. (2010); Grigoriev et al. (2010)). This result implies that detection of significant number of neutrons from TGFs is possible using the detector with effective area of about several hundred square centimeter. It means that above-described TGS instrument having minimal configuration of about 15 cm² effective area should be scaled up just in a few times.

Conclusions

A new project Universat-SOCRAT is proposed by Lomonosov Moscow State University based on the previous experience of TLE and TGF measurements from space. The successful realization of the project will make it possible to create a prototype of the space system for monitoring and warning of the space hazards for both ongoing and planned space missions, including high-altitude stratospheric aircrafts for the first time in the space exploration history. For the latter, it is especially actual to control the electromagnetic transients in the upper Earth's atmosphere and space (GRBs, solar flares), because such transient phenomena in the atmosphere as TGFs may be dangerous for aircrafts and for the planned sub-orbital missions.

Multi-wavelength synchronous observations with moderate accuracy of localization of TGF and TLE events give the unique information about high-energy processes in the Earth's atmosphere. Principally, it allows identification of TGF source with concrete thunderstorm area and significantly improving of probability of TGF identification with lightning. The last is crucial for testing of TAE theoretical models. Simultaneous observation of TGFs and TLEs can give information about peculiarities of high-altitude discharge, which is the most probable cause of these phenomena. Measurements of UV and optical emission of TLEs with high temporal resolution will continue investigation of serial flashes observed in Vernov and Lomonosov experiments. It will give information about spectrum and space-time structure of the events in thunderstorm and far from the thunderstorm regions.

Abbreviations

ASIC: Application-specific integrated circuit; DUV: Detector of ultraviolet; GRB: Gamma-ray burst; IR: Infrared; HV: High voltage; MAPMT: Multi-anode

photomultiplier tube MLT-S: Mini-lens telescope – spectrometer; MSU: Moscow State University; REB: Relativistic electron breakdown; RFB: Relativistic feedback discharge; RREA: Relativistic runaway electron avalanche; SiPM: Silicon photomultiplier; TAE: Transient atmospheric event; TGF: Terrestrial gamma-ray burst; TLE: Transient luminous event; UV: Ultraviolet; WWLLN: World Wide Lightning Location Network

Acknowledgements

Financial support for this work was provided by the Ministry of Education and Science of Russian Federation, Project # RFMEFI60717X0175.

Funding

This work was supported by the Ministry of Education and Science of Russian Federation, Project # RFMEFI60717X0175.

Availability of data and materials

Not applicable.

Authors' contributions

MP is a PI of Universat-SOCRAT experiment and author of general concept of the article. PK is a PI of the TUS Lomonosov and MLT-S Universat-SOCRAT experiments, and the main author of "Results of TLE observations in space experiments of Moscow State University" sections and "Instruments for TLE studies" of the article. SS is a PI of TGS and GFM Universat-SOCRAT experiments and the main author of "Introduction", "Results of TLE observations in space experiments of Moscow State University", "TGF observations in the Universat-SOCRAT project", and "Discussion and results" sections of the article. AB designed the MLT-S instrument electronic and is one of the authors of "Instruments for TLE studies" section intended for MLT-S description. VB designed the TGS instrument and is the author of "Tracking gamma-ray spectrometer" section of the article. AB is responsible for the data analysis and GFM instrument computer simulations, and is the author of "Gamma-ray flash monitor" section intended for GFM parameters. GG designed the UV spectrometer of MLT-S instrument electronic, and is one of the authors of "Instruments for TLE studies" section intended for MLT-S UV spectrometer description. AI is responsible for the analysis of neutron observations from the atmosphere, and is the author of the "The TLE and TGF study in other missions" section intended for neutron observations. MK carried out the TUS data analyses and collaborated with the corresponding author in the construction of the manuscript. IM designed the TDS instrument electronic and is one of the authors of "TGF observations in the Universat-SOCRAT project" section intended for TGS description. AM carried out the TGS computer simulations. AN provided the laboratory modeling of TGS units. PM collaborated in "The TLE and TGF study in other missions" section intended for optimization of TGF observations. VP is a project manager of Universat-SOCRAT experiment and is the author of "Concept of TLE and TGF observations in the Universat-SOCRAT project" section of the article. AP is an author of parts of "Introduction" and "The TLE and TGF study in other missions" sections intended for analysis of TGF study. YS carried out the laboratory modeling of MLT-S units. IY is an assistant of the project manager of Universat-SOCRAT experiment and is one of the authors of "Concept of TLE and TGF observations in the Universat-SOCRAT project" section intended for the instrument description. All authors read and approved the final manuscript.

Competing interests

The authors declare that they have no competing interest.

Publisher's Note

Springer Nature remains neutral with regard to jurisdictional claims in published maps and institutional affiliations.

Author details

¹Skobel'syn Institute of Nuclear Physics, Lomonosov Moscow State University, 1(2), Leninskie gory, Moscow 119991, Russia. ²Physics Department, Lomonosov Moscow State University, 1(2), Leninskie gory, Moscow 119991 Russia. ³Space Research Institute, Russian Academy of Science, 84/32 Profsoyuznaya Str, Moscow 117997 Russia. ⁴National Research University Higher School of Economics, 20 Myasnikinskaya Str, Moscow 101000 Russia.

Received: 7 September 2018 Accepted: 25 March 2019

Published online: 16 April 2019

References

- Armstrong R, Suszcynsky D, Lyons W, Nelson T (2000) Multi-color photometric measurements of ionization and energies in sprites. *Geophys Res Lett* 27(5):653–656
- Babich LP, Bochkov EI, Donskoi EN, Kutsyk IM (2010) Source of prolonged bursts of high-energy gamma rays detected in thunderstorm atmosphere in Japan at the coastal area of the sea of Japan and on high mountaintop. *J Geophys Res Space Phys* 115(A9):A09317. <https://doi.org/10.1029/2009JA015017>
- Babich LP, Bochkov EI, Kutsyk IM, Roussel-Dupré RA (2010) Localization of the source of terrestrial neutron bursts detected in thunderstorm atmosphere. *J Geophys Res Space Phys* 115:00–28
- Babich LP, Roussel-Dupré RA (2007) Origin of neutron flux increases observed in correlation with lightning. *J Geophys Res Atmos* 112(D13):D1330. <https://doi.org/10.1029/2006JD008340>
- Blin-Bondil S, Dulucq F, Rabanal J, Dagoret-Campagne S, Tongbong J, Barrillon P, de La Taille C, Moretto C, Miyamoto H, Thienpont D (2014) Spaciroc3: A front-end readout ASIC for JEM-EUSO cosmic ray observatory. *PoS* 172(TIPP2014)
- Bell TF, Pasko VP, Inan US (1995) Runaway electrons as a source of red sprites in the mesosphere. *Geophys Res Lett* 22(16):2127–2130
- Budtz-Jorgensen C, Kuvvetli I, Skogseide Y, Ullaland K, Ostgaard N (2009) Characterization of CZT detectors for the asim mission. *IEEE Trans Nucl Sci* 56(4):1842–1847
- Blanc E, Lefevre F, Roussel-Dupré R, Sauvaud J (2007) TARANIS: A microsatellite project dedicated to the study of impulsive transfers of energy between the earth atmosphere, the ionosphere, and the magnetosphere. *Adv Space Res* 40(8):1268–1275
- Boccippio D, R. Williams E, Heckman S, Lyons W, T. Baker I, Boldi R (1995) Sprites, elf transients, and positive ground strokes. *Science* 269:1088–1091
- Boeck WL, Vaughan OH, Blakeslee RJ, Vonnegut B, Brook M, McKune J (1995) Observations of lightning in the stratosphere. *J Geophys Res Atmos* 100(D1):1465–1475
- Bogomolov V, Panasyuk M, Svertilov S, Bogomolov A, Garipov G, Ilyudin A, Klimov P, Klimov S, Mishieva T, Minaev PY, et al. (2017) Observation of terrestrial gamma-ray flashes in the RELEC space experiment on the Vernov satellite. *Cosm Res* 55(3):159–168
- Briggs MS, Connaughton V, Wilson-Hodge C, Preece RD, Fishman GJ, Kippen RM, Bhat P, Pacias WS, Chaplin VL, Meegan CA, et al. (2011) Electron-positron beams from terrestrial lightning observed with Fermi GBM. *Geophys Res Lett* 38(2):L02808. <https://doi.org/10.1029/2010GL046259>
- Briggs MS, Xiong S, Connaughton V, Tierney D, Fitzpatrick G, Foley S, Grove JE, Chekhtman A, Gibby M, Fishman GJ, et al. (2013) Terrestrial gamma-ray flashes in the Fermi era: Improved observations and analysis methods. *J Geophys Res Space Phys* 118(6):3805–3830
- Briggs MS, Wersinger JM, Fogle Jr. M, Biaz S, Jenke P (2015) TRYAD: a pair of CubeSats to measure terrestrial gamma-ray flash beams. *AGU Fall Meet Abstr*:33–0481
- Capel F, Belov A, Casolino M, Klimov P (2018) Mini-EUSO: A high resolution detector for the study of terrestrial and cosmic UV emission from the International Space Station. *Adv Space Res* 62(10):2954–2965. <https://doi.org/10.1016/j.asr.2017.08.030>. Origins of Cosmic Rays
- Carlson B, Lehtinen NG, Inan US (2010) Neutron production in terrestrial gamma ray flashes. *J Geophys Res Space Phys* 115(A4):A00E19. <https://doi.org/10.1029/2009JA014696>
- Chern J, Hsu R, Su H-T, Mende S, Fukunishi H, Takahashi Y, Lee L-C (2003) Global survey of upper atmospheric transient luminous events on the ROCSAT-2 satellite. *J Atmos Solar-Terrestrial Phys* 65(5):647–659
- Christian H, Frost R, Gillaspay P, Goodman S, Vaughan Jr O, Brook M, Vonnegut B, Orville R (1983) Observations of optical lightning emissions from above thunderstorms using U-2 aircraft. *Bull Am Meteorol Soc* 64(2):120–123
- Christian H, Blakeslee R, Goodman S, Mach D, Stewart M, Buechler D, Koshak W, Hall J, Boeck W, Driscoll K, et al. (1999) The lightning imaging sensor. In: Proc. 11th Int. Conf. on Atmospheric Electricity, Guntersville, AL, ICAE. NASA. pp 746–749
- Cummer SA, Briggs MS, Dwyer JR, Xiong S, Connaughton V, Fishman GJ, Lu G, Lyu F, Solanki R (2014) The source altitude, electric current, and intrinsic brightness of terrestrial gamma ray flashes. *Geophys Res Lett* 41(23):8586–8593
- Drozdzov A, Amelushkin A, Bratolyubova-Tsulukidze L, Churilo I, Grigoriev A, Grigoryan O, Iudin D, Mareev E, Nechaev O, Petrov V (2010) Experiment based on spacesuit “Orlan-M”: Neutron fluxes from thunderstorms. *J Geophys Res Space Phys* 115(A8):A00E51
- Dwyer JR (2007) Relativistic breakdown in planetary atmospheres. *Phys Plasmas* 14(4):042901
- Dwyer JR, Grefenstette BW, Smith DM (2008) High-energy electron beams launched into space by thunderstorms. *Geophys Res Lett* 35(2):L02815. <https://doi.org/10.1029/2007GL032430>
- Dwyer JR, Smith DM, Cummer SA (2012) High-energy atmospheric physics: Terrestrial gamma-ray flashes and related phenomena. *Space Sci Rev* 173(1–4):133–196
- Enoto T, Wada Y, Furuta Y, Nakazawa K, Yuasa T, Okuda K, Makishima K, Sato M, Sato Y, Nakano T, et al. (2017) Photonuclear reactions triggered by lightning discharge. *Nature* 551(7681):481
- Farges T, Hébert P, Le Mer-Dachard F, Ravel K, Gaillac S (2017) Microcameras and photometers (MCP) on board the TARANIS satellite. In: AGU Fall Meeting Abstracts. abstract #AE21A-04
- Fisher JR (1990) Upward discharges above thunderstorms. *Weather* 45(12):451–452
- Fishman GJ, Bhat P, Mallozzi R, Horack J, Koshut T, Kouveliotou C, Pendleton G, Meegan C, Wilson R, Pacias W, et al. (1994) Discovery of intense gamma-ray flashes of atmospheric origin. *Science* 264(5163):1313–1316
- Fukunishi H, Takahashi Y, Kubota M, Sakanoi K, Inan US, Lyons WA (1996) Elves: Lightning-induced transient luminous events in the lower ionosphere. *Geophys Res Lett* 23(16):2157–2160. <https://doi.org/10.1029/96GL01979>
- Fuquay DM, Baughman RG, Taylor AR, Howe RG (1967) Characteristics of seven lightning discharges that caused forest fires. *J Geophys Res* 72(24):6371–6373
- Garipov G, Khrenov B, Panasyuk M, Tulupov V, Shirokov A, Yashin I, Salazar H (2005) UV radiation from the atmosphere: results of the msu “Tatiana” satellite measurements. *Astropart Phys* 24(4–5):400–408
- Garipov G, Panasyuk M, Rubinshtein I, Tulupov V, Khrenov B, Shirokov A, Yashin I, Salazar H (2006) Ultraviolet radiation detector of the MSU research educational microsatellite Universitetskii-Tat’iana. *Instrum Exp Tech* 49(1):126–131
- Garipov G, Khrenov B, Klimov P, Klimenko V, Mareev E, Martines O, Mendoza E, Morozenko V, Panasyuk M, Park I, et al. (2013) Global transients in ultraviolet and red-infrared ranges from data of Universitetskyy-Tatiana-2 satellite. *J Geophys Res Atmos* 118(2):370–379
- Grigoriev A, Grigoryan O, Drozdov AY, Malyskin Y, Popov Y, Mareev E, Iudin D (2010) Thunderstorm neutrons in near space: analyses and numerical simulation. *J Geophys Res Space Phys* 115(A8):A00E52. <https://doi.org/10.1029/2009JA014870>
- Gurevich A, Milikh G, Roussel-Dupre R (1992) Runaway electron mechanism of air breakdown and preconditioning during a thunderstorm. *Phys Lett A* 165(5–6):463–468
- Iwanowska J, Swiderski L, Szczesniak T, Sibczynski P, Moszynski M, Grodzicka M, Kamada K, Tsutsumi K, Usuki Y, Yanagida T, et al. (2013) Performance of cerium-doped Gd3Al2Ga3O12 (GAGG: Ce) scintillator in gamma-ray spectrometry. *Nucl Inst Methods Phys Res Sect A: Accelerators, Spectrometers, Detectors Assoc Equip* 712:34–40
- Ilyudin A, Bogomolov V, Galkin V, Golovanov I, Krasnov A, Markelova A, Markelov I, Morgunova Y, Osedlo V, Panasyuk M, et al. (2015) Instruments to study fast neutrons fluxes in the upper atmosphere with the use of high-altitude balloons. *Adv Space Res* 56(10):2073–2079
- Khrenov B, Klimov P, Panasyuk M, Sharakin S, Tkachev L, Zotov MY, Biktemerova S, Botvinko A, Chirskaya N, Ereemeev V, et al. (2017) First results from the TUS orbital detector in the extensive air shower mode. *J Cosmol Astropart Phys* 2017(09):006
- Klimov P, Garipov G, Khrenov B, Morozenko V, Barinova V, Bogomolov V, Kaznacheeva M, Panasyuk M, Saleev K, Svertilov S (2017) Vernov satellite data of transient atmospheric events. *J Appl Meteorol Climatol* 56(8):2189–2201
- Klimov P, Panasyuk M, Khrenov B, Garipov G, Kalmykov N, Petrov V, Sharakin S, Shirokov A, Yashin I, Zotov M. Y, et al (2017) The TUS detector of extreme energy cosmic rays on board the Lomonosov satellite. *Space Sci Rev* 212(3–4):1687–1703
- Klimov P, Kaznacheeva M, Khrenov B, Garipov G, Bogomolov V, Panasyuk M, Svertilov S, Cremonini R (2018) UV transient atmospheric events observed far from thunderstorms by the Vernov satellite. *IEEE Geosci Remote Sens Lett* 15(8):1139–1143
- Lehtinen NG, Bell TF, Pasko V, Inan U (1997) A two-dimensional model of runaway electron beams driven by quasi-electrostatic thundercloud fields. *Geophys Res Lett* 24(21):2639–2642

- Lyons WA (1994) Characteristics of luminous structures in the stratosphere above thunderstorms as imaged by low-light video. *Geophys Res Lett* 21(10):875–878
- Mazets EP, Golenetskii SV (1981) Recent results from the gamma-ray burst studies in the KONUS experiment. *Astrophys Space Sci* 75:47–81
- Milikh G, Valdivia J, Papadopoulos K (1998) Spectrum of red sprites. *J Atmos Solar-Terrestrial Phys* 60(7–9):907–915
- Minaev PY, Pozanenko A, Molkov S, Grebenev S (2014) Catalog of short gamma-ray transients detected in the SPI/INTEGRAL experiment. *Astron Lett* 40(5):235–267
- Minaev P, Pozanenko A (2018) Search for short transient gamma-ray events in SPI experiment onboard INTEGRAL: The algorithm and results. In: Kalinichenko L, Manolopoulos Y, Malkov O, Skvortsov N, Stupnikov S, Sukhomlin V (eds). *Data Analytics and Management in Data Intensive Domains*. Springer, Cham, pp 128–138
- Moos RH, Moos BS (2006) Rates and predictors of relapse after natural and treated remission from alcohol use disorders. *Addiction* 101(2):212–222
- Neubert T, Kuvvetli I, Budtz-Jørgensen C, Østgaard N, Reglero V, Arnold N (2006) The atmosphere-space interactions monitor (ASIM) for the international space station. In: ILWS (International Living With a Star) Workshop. pp 19–20
- Orville RE, Henderson RW (1984) Absolute Spectral Irradiance Measurements of Lightning from 375 to 880 nm. *J Atmos Sci* 41:3180–3180
- Østgaard N, Gjesteland T, Stadsnes J, Connell P, Carlson B (2008) Production altitude and time delays of the terrestrial gamma flashes: Revisiting the burst and transient source experiment spectra. *J Geophys Res Space Phys* 113(A2):A02307. <https://doi.org/10.1029/2007JA012618>
- Panasyuk M, Svertilov S, Bogomolov V, Garipov G, Barinova V, Bogomolov A, Veden'kin N, Golovanov I, Iyudin A, Kalegaev V, et al (2016a) Experiment on the Vernov satellite: Transient energetic processes in the Earth's atmosphere and magnetosphere. Part I: Description of the experiment. *Cosm Res* 54(4):261–269
- Panasyuk M, Svertilov S, Bogomolov V, Garipov G, Barinova V, Bogomolov A, Veden'kin N, Golovanov I, Iyudin A, Kalegaev V, et al. (2016b) Experiment on the Vernov satellite: transient energetic processes in the Earth's atmosphere and magnetosphere. Part II, First results. *Cosm Res* 54(5):343–350
- Panasyuk M, Podzolkov M, Kovtyukh A, Brilkov I, Vlasova N, Kalegaev V, Osedlo V, Tulupov V, Yashin I (2015) Operational radiation monitoring in near-earth space based on the system of multiple small satellites. *Cosm Res* 53(6):423–429
- Panasyuk M, Podzolkov M, Kovtyukh A, Brilkov I, Vlasova N, Kalegaev V, Osedlo V, Tulupov V, Yashin I (2017) Optimization of measurements of the Earth's radiation belt particle fluxes. *Cosm Res* 55(2):79–87
- Pasko VP, Yair Y, Kuo C-L (2012) Lightning related transient luminous events at high altitude in the Earth's atmosphere: phenomenology, mechanisms and effects. *Space Sci Rev* 168:475–516. <https://doi.org/10.1007/s11214-011-9813-9>
- Roberts OJ, Fitzpatrick G, Stanbro M, McBreen S, Briggs MS, Holzworth RH, Grove JE, Chekhtman A, Cramer ES, Mailyan BG (2018) The first Fermi-GBM terrestrial gamma ray flash catalog. *J Geophys Res Space Phys* 123(5):4381–4401. <https://doi.org/10.1029/2017JA024837>. <https://agupubs.onlinelibrary.wiley.com/doi/pdf/10.1029/2017JA024837>
- Sadovnichy V, Panasyuk M, Bobrovnikov SY, Vedenkin N, Vlasova N, Garipov G, Grigorian O, Ivanova T, Kalegaev V, Klimov P, et al. (2007) First results of investigating the space environment onboard the Universitetskii-Tatyana satellite. *Cosm Res* 45(4):273–286
- Sadovnichy V, Panasyuk M, Yashin I, Barinova V, Veden'kin N, Vlasova N, Garipov G, Grigoryan O, Ivanova T, Kalegaev V, et al (2011) Investigations of the space environment aboard the Universitetskii-Tat'yana and Universitetskii-Tat'yana-2 microsatellites. *Sol Syst Res* 45(1):3–29
- Sadovnichy V, Panasyuk M, Amelyushkin A, Bogomolov V, Benghin V, Garipov G, Kalegaev V, Klimov P, Khrenov B, Petrov V, et al (2017) "Lomonosov" satellite—space observatory to study extreme phenomena in space. *Space Sci Rev* 212(3–4):1705–1738
- Sarria D, Lebrun F, Blély P-L, Chipaux R, Laurent P, Sauvaud J-A, Prech L, Devoto P, Pailot D, Baronick J-P, et al (2017) TARANIS XGRE and IDEE detection capability of terrestrial gamma-ray flashes and associated electron beams. *Geosci Instrum Methods Data Syst* 6(2):239–256
- Sato M, Adachi T, Ushio T, Morimoto T, Kikuchi M, Kikuchi H, Suzuki M, Yamazaki A, Takahashi Y, Ishida R, Sakamoto Y, Yoshida K, Hobara Y (2017) Sprites identification and their spatial distributions in JEM-GLIMS nadir observations. *Terr Atmos Ocean Sci* 28:545–561. <https://doi.org/10.1029/96GL01979>
- Sharkov EA, Kuzmin AV, et al. (2018) Space experiment "Convergence": scientific objectives, on-board equipment, methods of reverse problems. *Izv. Atm. Ocean Phys* 54(9):71–96
- Shibata S (1994) Propagation of solar neutrons through the atmosphere of the Earth. *J Geophys Res Space Phys* 99(A4):6651–6665
- Smith DM, Lopez LI, Lin RP, Barrington-Leigh CP (2005) Terrestrial gamma-ray flashes observed up to 20 MeV. *Science* 307(5712):1085–1088
- Svertilov S, Panasyuk M, Bogomolov V, Amelushkin A, Barinova V, Galkin V, Iyudin A, Kuznetsova E, Prokhorov A, Petrov V, et al (2018) Wide-field gamma-spectrometer BDRG: GRB monitor on-board the Lomonosov mission. *Space Sci Rev* 214(1):8
- Tavani M, Marisaldi M, Labanti C, Fuschino F, Argan A, Trois A, Giommi P, Colafrancesco S, Pittori C, Palma F, et al (2011) Terrestrial gamma-ray flashes as powerful particle accelerators. *Phys Rev Lett* 106(1):018501
- Tierney D, Briggs M, Fitzpatrick G, Chaplin V, Foley S, McBreen S, Connaughton V, Xiong S, Byrne D, Carr M, et al (2013) Fluence distribution of terrestrial gamma ray flashes observed by the Fermi Gamma-ray Burst Monitor. *J Geophys Res Space Phys* 118(10):6644–6650
- Ushio T, Sato M, Morimoto T, Suzuki M, Kikuchi H, Yamazaki A, Takahashi Y, Hobara Y, Inan U, Linscott I, et al (2011) The global lightning and sprite measurement (GLIMS) mission on International Space Station. *IEEJ Trans Fundam Mater* 131(12):971–976
- Vaughan O, Vonnegut B (1989) Recent observations of lightning discharges from the top of a thundercloud into the clear air above. *J Geophys Res Atmos* 94(D11):13179–13182
- Vedenkin N, Garipov G, Klimov P, Klimenko V, Mareev E, Martinez O, Morozenko V, Park I, Panasyuk M, Ponce E, et al (2011) Atmospheric ultraviolet and red-infrared flashes from Universitetskii-Tat'yana-2 satellite data. *J Exp Theor Phys* 113(5):781–790
- Winckler J, Lyons W, Nelson T, Nemzek R (1996) New high-resolution ground-based studies of sprites. *J Geophys Res Atmos* 101(D3):6997–7004
- Zoglauer AC (2005) First light for the next generation of Compton and pair telescopes. PhD thesis. Technische Universität München
- Zoglauer A, Andritschke R, Schopper F (2006) MEGALib—the medium energy gamma-ray astronomy library. *New Astron Rev* 50(7–8):629–632

Submit your manuscript to a SpringerOpen® journal and benefit from:

- Convenient online submission
- Rigorous peer review
- Open access: articles freely available online
- High visibility within the field
- Retaining the copyright to your article

Submit your next manuscript at ► [springeropen.com](https://www.springeropen.com)